Temperature dependence of Raman scattering from the high-pressure phases of Si induced by indentation

B. C. Johnson,[1,*,†] B. Haberl,[2] J. E. Bradby,[2] J. C. McCallum,[1] and J. S. Williams[2]

[1]*School of Physics, The University of Melbourne, Victoria 3010, Australia*

[2]*Department of Electronic Materials Engineering, Research School of Physics and Engineering, The Australian National University, Canberra ACT 0200, Australia*

(Received 13 February 2011; revised manuscript received 23 April 2011; published 6 June 2011)

A micro-Raman scattering study on the linewidth and frequency shift of Si-III and Si-XII produced by indentation is presented over the temperature range 80–300 K. Measurements are compared to the Raman lines originating from the Si-I substrate. The main Si-XII Raman line shows a strong dependence on temperature and can be adequately described by anharmonic terms from the phonon proper self-energy. In contrast, the main Si-III Raman linewidth decreases with increasing temperature. A model related to electron-phonon interactions describes the data well.

DOI: 10.1103/PhysRevB.83.235205 PACS number(s): 78.30.Am, 63.22.Kn, 64.60.My

I. INTRODUCTION

The metastable high-pressure phases of silicon have attracted much attention since they can be easily integrated into existing Si technologies in which their alternative properties can be utilized.[1] During indentation, the diamond cubic phase, Si-I, transforms to the metallic β-Sn phase, Si-II. This phase is not stable at ambient pressures. If the pressure is released slowly, Si-II transforms into a mixture of the polycrystalline high-pressure phases Si-XII (semiconductor,[2,3] $r8$, $a = 5.609$ Å, and $\gamma = 110.07$),[4] and Si-III (semimetal,[5,6] $bc8$, $a = 3.80$ Å, and $c = 6.28$ Å).[7] A fast pressure release is likely to result in a transformation to amorphous silicon (a-Si).[8] A hexagonal diamond phase, Si-IV, has been reported after heating Si-III above 450 K.[5,6] In all, there are 13 identified phases of Si each with unique structures and properties, and they are summarized in Table I.

Raman spectroscopy has provided an indispensable and sensitive tool for characterizing these phases and their transformations. Some phases (such as Si-III and Si-XII) are metastable at ambient pressures and temperatures and these can be identified from their unique Raman spectrum, but since the Si-XII structure is closely related to that of Si-III, their Raman spectra are somewhat similar. Furthermore, these two phases often coexist in indents and the calculated zone-center phonon frequencies differ by only 10%, making phonon mode assignments to the Raman line of one particular phase difficult.[18] Indeed, a repressurization diamond anvil cell study of the high-pressure phases was not able to distinguish between Si-III and Si-XII lines unambiguously.[21] Temperature studies may serve as a guide to the proper identification of Si-III and Si-XII in indentation samples and also to the properties of the various phonons involved. For Si-I, the width of the Raman line is an important physical parameter as it reflects the anharmonic interaction of the Raman-active optical phonons decaying into combinations of lower-energy phonons.[22–24] The temperature dependence of the optical mode has revealed much about the nature of phonons and mechanisms that affect their lifetime.[25–29] Such studies have also allowed Raman lines to be used as a convenient probe of the temperature profile of heated silicon, germanium, and diamond as well as a growing number of other materials. The temperature dependence of the high-pressure phases of Si has yet to be examined.

Here, we have examined the various Raman lines characteristic of Si-III and Si-XII formed by indentation from 80 K up to room temperature—well below the temperatures at which temperature-induced phase transformation effects may occur. The study reveals that the dominant Si-XII Raman line (351.9 cm^{-1}) is governed by the anharmonicity of the Si-XII lattice. Semiempirical relations can be used to describe the frequency shift and dampening of this line similar to that for Si-I. In contrast, the dominant Raman line of Si-III (437.5 cm^{-1}) displays a unique trend where the linewidth decreases with increasing temperature. These observations are discussed in the context of standard anharmonic theories, and alternative explanations for the Si-III phonon behavior are explored.

II. BACKGROUND

In many systems, the temperature dependence of the Raman line is governed by the anharmonic potential in which the atoms of the lattice vibrate. As the temperature increases, the anharmonicity leads to an increase in phonon-phonon interactions. This in turn results in scattering and shorter optical phonon lifetimes and is accompanied by an increase in the acoustic phonon population. Hence, in many systems the width of the Raman line increases with temperature. The linewidth, Γ, and the phonon lifetime, τ, can be related by the energy-time uncertainty relation, $\Gamma/\hbar = 1/\tau$.[30] Raman spectroscopy then can be used as a simple, albeit indirect, method to determine the phonon lifetime. In addition to the linewidth broadening, the Raman line frequency also shifts with temperature following from anharmonic terms in the vibrational Hamiltonian of the crystal lattice and can be expressed as[25]

$$\Omega(T) = \Omega_o + \Delta_a(T) + \Delta_e(T), \tag{1}$$

where Ω_o is the harmonic mode of the phonon, Δ_a is the shift due to the decay of optical phonons into phonons of lower energy (anharmonic terms), and Δ_e is the shift due to thermal expansion. By taking into account cubic and quartic terms in

TABLE I. Summary of the known Si phases.

Phase	Structure	Production	References
Si-I	Diamond-cubic		9
Si-II	Body-centered-tetragonal (β-Sn)	$\sim$11 GPa	10 and 11
Si-III	Body-centered-cubic ($bc8$)	Decompression from Si-XII at $\sim$3.2 GPa	7 and 12
Si-IV	Hexagonal-diamond	annealing of Si-III at 200–600 °C	5 and 6
Si-V	Simple-hexagonal	15.4 GPa	13 and 14
Si-VI	Orthorhombic($Cmca$)	$\sim$38 GPa	15
Si-VII	Hexagonal-close-packed	42 GPa	16
Si-VIII	Tetragonal-30	Rapid decompression from 14.8 GPa	17
Si-IX	Tetragonal-12	Rapid decompression from 12.0 GPa	17
Si-X	Face-centered-cubic	79–248 GPa	16
Si-XI	Body-centered-orthorhombic ($Imma$)	$\sim$13 GPa	13 and 14
Si-XII	Rhombohedral ($r8$)	Slow decompression of Si-II from 10 GPa	4 and 18
Si-XIII	Unknown	Annealing of Si-III/Si-XII	19
a-Si	Amorphous	Fast pressure release	20

the anharmonic Hamiltonian and considering only symmetric decays of the zone-center phonons into two phonons (third-order process) and three phonons (fourth-order process), the Δ_a term is given by[27]

$$\Delta_a = A[1 + 2n(T,\Omega_o/2)] + B[1 + 3n(T,\Omega_o/3) + 3n^2(T,\Omega_o/3)], \quad (2)$$

where $n(T,\omega) = [\exp(\hbar\omega/k_bT)]^{-1}$ is the Bose-Einstein distribution function and A and B are anharmonic constants for three- and four-phonon processes, respectively. Temperature-dependent thermal expansion coefficients and the mode Grüneisen parameter are contained in Δ_e. For Si-I it has been suggested that the thermal expansion contribution cancels with a quartic anharmonic term and is therefore often ignored.[31] In any case, these parameters are not known for Si-III and Si-XII and so a theoretical calculation of the Raman shift for these phases is not yet possible. At $T = 0$ K, the frequency of the Raman mode is $\Omega(0) = \omega_o = \Omega_o + \Delta_a(0) + \Delta_e(0) \approx \Omega_o + A + B$. The linewidth due to the anharmonicity is likewise given by

$$\Gamma(T) = C[1 + 2n(T,\Omega_o/2)] + D[1 + 3n(T,\Omega_o/3) + 3n^2(T,\Omega_o/3)], \quad (3)$$

where C and D are the linewidth counterparts of A and B in Eq. (2). The zero-temperature linewidth is $\Gamma_o = C + D$ but may also contain additional temperature-independent inhomogeneous broadening terms arising from phonon scattering at grain boundaries and defects. In addition, it has been noted that there is wide variability in the reported values for Γ_o in Si, Ge, and diamond.[25] This is mostly due to the finite resolution of the spectrometer. Ulrich *et al*. have measured a corrected value of $\Gamma_o = 1.08$ cm^{-1} for Si-I.[22] This corresponds to a lifetime of 4.92 ps.

The temperature dependence of a Raman line can be treated to various degrees of complexity. The Klemens model, which considers only three-phonon processes where optical phonons decay into two acoustic phonons of the same frequency [the first terms in Eq. (1) and (3)],[32] can adequately describe the first-order diamond line for example.[33] However, Cui *et al*. has described deviations between the model and the diamond line position at temperatures of 600 and 1600 K.[34] This has led them to propose a purely empirical relationship. For temperatures above 600 K, Si-I requires the quartic anharmonic contribution to be invoked to capture the temperature dependence accurately [the second terms in Eqs. (2) and (3), which vary quadratically with T].[27] The $\Delta_e(T)$ term in Eq. (1) has also been used [in addition to $\Delta_a(T)$] to describe the temperature variation in Si-I and Ge-I up to the melting point.[35] Unless one of these terms is determined independently, it is difficult to deconvolute their contributions solely with Raman spectroscopy.

A number of other effects can act to modify the Raman line shape arising from electron-phonon (e-p) coupling where vibrational energy is dissipated into electronic excitations or vice versa. Fano-type asymmetric broadening[36] can occur via the coupling of a phonon mode with a broad electronic continuum such as is observed when phonons interact with free carriers or with intraband transitions in the valence or conduction bands.[37,38] Raman linewidth broadening can also be governed by the e-p coupling strength as in Allen's formalism.[39–41] This effect will be discussed further below when discussing the Si-III results.

In the following, we show that the Raman lines of Si-III and Si-XII have a strong temperature dependence. Using the theoretical framework outlined above, phonons governed by the anharmonicity of the lattice are identified and described with anharmonic constants. Notably, the most prominent Raman line of Si-III cannot be described with these models.

Instead, an empirical model is proposed and possible physical explanations are explored.

III. EXPERIMENT

An array of 64 indents was formed in Czochralski grown Si(100) wafers, p-doped with boron to a resistivity of 8–10 Ω cm using an Ultra-Micro-Indentation-System 2000 equipped with an ∼17 μm radius spherical indenter tip. A maximum load of 750 mN was used with the unloading performed in 200 increments (average unload rate ∼1.3 mN/s). This ensured that a pop-out event occurred on unloading, indicating that the phase transformed zone (of spot size around 10 μm in diameter with a maximum depth of 400 nm) contained the high-pressure crystalline phases (Si-III and Si-XII).[8] Small volumes of a-Si are also present.

The 532 nm line of an Ar-ion laser was focused onto the middle of the indent with a confocal microscope in a backscattering geometry. A 20×, long working distance objective lens with a numerical aperture of 0.4 resulted in an ∼5 μm laser spot size and was used for all measurements. A Linkam temperature stage (THMS600) with a quartz window was used to heat the sample between 80 and 300 K in a flowing nitrogen atmosphere. The Si-I related Raman lines were measured up to a temperature of 570 K. The temperature stability was estimated to be within 1 K. For each measurement point, the temperature was stabilized for a few minutes before acquiring a spectrum for 200 s with a Renishaw InVia Reflex 0.25 working distance micro-Raman spectrometer with a 2400 grooves/mm grating. The laser power was kept at a level where the indents were not affected by any unintentional laser heating (5 mW as measured after the objective corresponding to a laser power of approximately 6 kW/cm^2 at the sample surface). We note that for shorter laser wavelengths (such as 514 nm), laser heating becomes a significant issue for these indents. The Si-I peak at 520.3 cm^{-1} was found to dominate all the spectra measured. This indicates that the penetration depth of the 532 nm laser is beyond the transformed volume and hence only a small fraction of the laser energy is absorbed in the near-surface region. Taking into account variations between each indent and the intrinsic instrument error, the overall wave-number error was estimated to be ±0.5 cm^{-1} at any given temperature. The spectral resolution of the setup was 1.1 cm^{-1} per CCD pixel for a 2400 mm^{-1} grating. However, by using a fitting routine discussed below, a nominal subpixel resolution of 0.1 cm^{-1} could be achieved.

Within the transformed zone, crystallite sizes are expected to be on average ∼5–30 nm in diameter as determined from transmission electron microscopy measurements.[42] In addition to phonon confinement effects, which cause an asymmetry in the Raman line,[43] anharmonic constants such as C in Eq. (3) have been observed to increase asymptotically with a decrease in nanocrystalline Si-I size for diameters < 7 nm.[44] Consequently, the temperature dependence of nanocrystalline Si-I deviates from the bulk value since the anharmonicity of the crystal increases with decreasing crystal size. No asymmetry is observed in the Si-III and -XII Raman lines studied here. However, it should be noted that the distribution in crystal sizes may result in Raman line broadening. Variations of the anharmonicity arising from phonon confinement are neglected. Stress may also contribute to temperature-independent inhomogeneous broadening effects. We have limited the temperature over which the indents were analyzed to avoid any temperature-induced phase transformations that may affect the stress fields inside the indent.

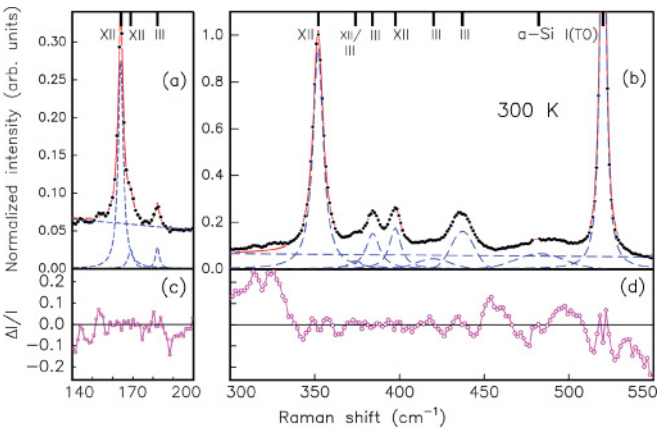

FIG. 1. (Color online) Raman spectra of an indent in the wave-number range (a) 140–200 cm^{-1} and (b) 300–550 cm^{-1} collected with a 532 nm laser for 200 s at 300 K. The intensity has been normalized to the intensity of the main Si-XII line at 351.9 cm^{-1}. The tick marks at the top of each panel indicate the position of the centroids for each curve used in the fit. The lower panels (c) and (d) show the residual errors.

IV. RESULTS AND DISCUSSION

Figure 1 shows a typical Raman spectrum from indented Si taken at 300 K. All peaks are fitted with Lorentzians except for the main Si-III peak (at 437.5 cm^{-1}), which was better described by a Gaussian line shape. Gaussian Raman lines are often associated with broadening due to structural disorder.[45] Here, the Gaussian line shape of the main Si-III line may indicate that the phase exhibits short-range disorder, possibly arising from angular distortions in the tetrahedral bonds as described by Kasper *et al.*[46] and Kobliska *et al.*[47] for Si-III. The transverse optic (TO), longitudinal acoustic, and longitudinal optic Raman modes of a-Si were fitted by a single Gaussian to minimize the parameters used in the fit. This gives rise to some discrepancy as shown in the residual error [Fig. 1(b)]. An additional Gaussian was required to fit a small feature at around 420 cm^{-1} in this figure, which becomes more evident after laser heating (not shown). In fitting the data, the linewidth of the small Si-III/XII line at 373 cm^{-1} was kept at a value of 7.08 cm^{-1} to reduce the number of variables. The natural linewidth of the Raman lines was extracted by fitting the Si-I peak with a pseudo-Voigt function. The broadening resulting from the spectrometer response was determined to be (0.4 ± 0.2) cm^{-1}. The Γ values presented below are the corrected values (deconvoluted from the spectrometer broadening) and therefore represent the natural linewidth rather than the spectrometer broadened linewidth.

The Ω values of the Si-III and Si-XII related Raman lines at 20 °C are listed in Table II. Associated phonons are given in parentheses following the assignments of

TABLE II. Raman lines of the different phases of silicon observed at 20 °C. The Ω ($T = 20$ °C) values were determined using Eq. (1) with parameters determined in this work. The main Si-I, -XII, and -III lines are underlined. The phonon modes are assigned following theoretical calculations in Ref. 18.

Ω (cm^{-1})	Phase (phonon)	Structure	References
~150 (broad)	*a*-Si (TA)	amorphous	45
164.8	Si-XII (A_g)	*r*8	
170.0	Si-XII (E_g)		
182.4	Si-III (T_g)	*bc*8	47
301.9	Si-I [2TA(*X*)]	dc	48 and 49
351.9	Si-XII (A_g)	*r*8	18,50, and 51
373.3	Si-III/Si-XII	*bc*8/*r*8	52
384.2	Si-III (T_g)	*bc*8	47 and 51
397.1	Si-XII	*r*8	18,50, and 51
412	Si-III	*bc*8	47 and 51
437.5	Si-III (E_u)	*bc*8	47 and 51
463	Si-III (E_g)	*bc*8	47
~470 (broad)	*a*-Si (TO/LO/LA)	amorphous	45
520.3	Si-I (TO)	dc	48 and 49

Piltz *et al.*[18] The corresponding crystal structure type and additional references are also shown. For the case of Si-III,[18,47] no Raman line is theoretically calculated below 180 cm^{-1}. Therefore, the line at 167.7 cm^{-1} is assigned to Si-XII. Furthermore, although the theoretical calculations for Si-XII[18] yield Raman lines at slightly higher wave numbers than 164.8 cm^{-1}, the calculation[18] of the two lowest Si-XII modes at 178.1(A_g) and 182.5 cm^{-1}(E_g) appear to match the two low-frequency modes observed. The line at 182.4 cm^{-1} has not been previously assigned conclusively. However, it agrees well with the lowest Si-III mode calculated by Piltz *et al.* at 186.8 cm^{-1}(T_g) (Ref. 18) and Kobliska *et al.* at 181 cm^{-1}.[47] Therefore, this line here is assigned to Si-III. It is not possible to unambiguously assign the line at 373.2 cm^{-1} as it does not match any of the Si-III or Si-XII modes calculated by Piltz *et al.*[18] Furthermore, this line seems to be very pressure-dependent with a significantly higher intensity observed at increased pressures in a diamond-anvil cell,[21] which might warrant an assignment as Si-XII. However, its presence also seems to correlate to the presence of the Si-III line at 182.4 cm^{-1}, making a definitive assignment difficult. We also note that the representative Raman spectrum in Fig. 1 is very similar to the spectrum observed by Olijnyk *et al.* in a diamond anvil cell after pressure release to a 1.7 GPa load.[21] The spectrum is in fact noticeably different from the ambient pressure spectrum. This suggests that there are residual stress effects contained in the indents studied here.

Figure 2 shows the Raman spectra over three wave-number ranges of interest for measurement temperatures between 80 and 300 K. A downward shift and an intensity decrease are evident in all of the observed Raman lines with increasing temperature. In Fig. 2(c), the *a*-Si peak can be detected at ~500 cm^{-1}. In an early work, the transverse optic (TO) Raman line of *a*-Si prepared by ion implantation was shown not to have a temperature dependence.[53] To verify this, we also measured an indent formed by fast indentation unloading, which resulted in only the pressure-induced *a*-Si phase. This allowed the

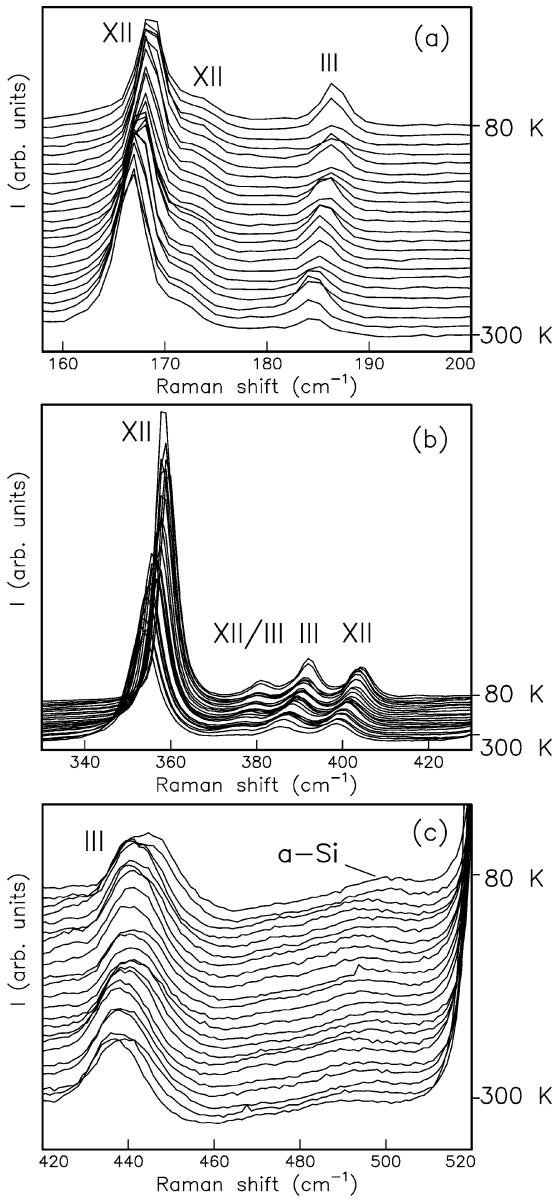

FIG. 2. Raman spectra of the indent as a function of temperature in three different wave-number regions. The spectra have been offset vertically for clarity with the 80 K spectra at the top as indicated along the right axis. The roman numerals indicate the Si phase.

Raman signal of *a*-Si to be easily identified. In contrast to this previous work on *a*-Si formed by ion implantation, a downward shift in the frequency between 80 K and room temperature was found to be ~10 cm^{-1} for pressure-induced *a*-Si. This seems to be consistent with an anharmonic effect and may be described by Eq. (1). Furthermore, this observation is in fair agreement with later measurements made on deposited *a*-Si.[54] There are clear differences in *a*-Si fabricated by ion implantation, indentation, or deposition. These discrepancies in the Raman line behavior might therefore be expected. However, a systematic comparison has not yet been performed. In the indents under study here, we expect a similar shift in the *a*-Si peak to that observed in our *a*-Si indent.

Figure 3 shows the Raman frequency shift relative to ω_o [Fig. 3(a)] and the corrected linewidth [Fig. 3(b)] as a function

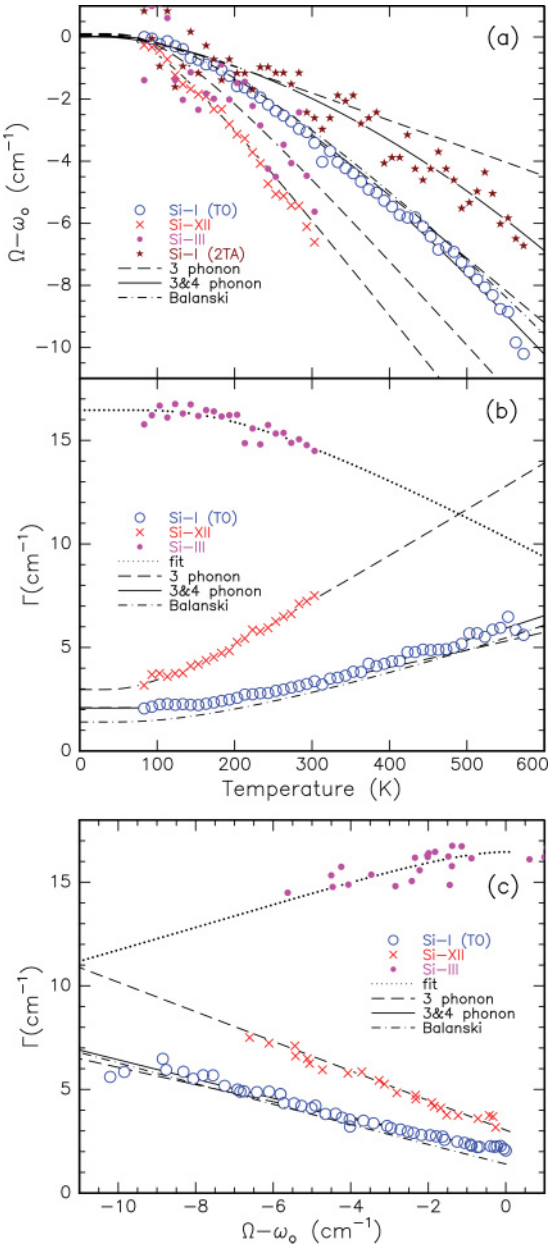

FIG. 3. (Color online) (a) Raman frequency shift relative to ω_o and (b) the corrected linewidth as a function of temperature for the main Si-I, Si-III, and Si-XII lines (520.3, 437.7, and 351.9 cm^{-1} in Table II, respectively), and (c) the linewidth vs the line shift. The lines are fits using Eqs. (2) and (3) for Si-I and -XII. Solid lines and dashed lines represent the equations with and without the higher-order terms, respectively. The Si-III Γ data are fit with Eq. (4) (dotted line). Fits using Eqs. (2) and (3) from Balkanski *et al*. are shown for comparison (dash-dotted line).[27]

of temperature for the main Si-I, Si-III, and Si-XII lines. The data set for Si-I and Si-XII have been fitted using Eqs. (2) and (3). The results of these fits are collated in Table III. The errors quoted in the table are determined from chi-square at convergence of the fit.

Figure 3(c) shows the corrected linewidth versus the frequency shift for the data and fits obtained from Figs. 3(a) and 3(b). Within error, the data show a linear dependence over the temperature range considered. The fits with the three-phonon process are essentially linear given that the temperature dependence of the Ω_a and Γ terms are similar. The four-phonon process (for Si-I) results in a slight nonlinear trend that is not apparent over the temperature range considered. These trends suggest that the phonons are indeed described well by the Kramers-Kronig relation. That is, the observed trends are a result of the anharmonicity of the lattice. The more obvious nonlinear trend observed for Si-III suggests that other effects are operative, and these are discussed below. The Si-I TO and second-order transverse acoustic (2TA) lines and the main Si-XII (351.9 cm^{-1}) and Si-III (437.7 cm^{-1}) Raman lines are discussed in turn below.

In Fig. 3, both the three-phonon and the four-phonon models have been used to fit the Si-I data [Eqs. (2) and (3) with the higher-order term omitted or included]. For the Si-I TO line, there is a slight deviation as the temperature reaches above 500 K. As mentioned earlier, four-phonon processes are known to be required to model this line accurately at temperatures above 600 K.[27] The corrected Si-I TO linewidth in Fig. 3(b) is 0.5 cm^{-1} broader on average than that determined by Balkanski *et al*.[27] This may be expected of our system where phonon lifetimes can be shortened by scattering at defects and the Si-I/transformed region interface. The ratios B/A and D/C for the Si-I TO Raman line are $B/A = 0.05$ and $D/C = 0.01$. These are smaller than those determined by Balkanski *et al*. ($B/A = 0.08$ and $D/C = 0.06$).[27] This is most likely a result of the lower-temperature range over which the model was fitted to the data in our case. Only at higher temperatures do four-phonon processes become noticeable.

The temperature dependence of the Si-I 2TA line shift has also been determined in the Si-I substrate and is shown for comparison. The TO phonon originates from the center of the Brillouin zone, whereas the 2TA phonon comes from the boundary point X of the Brillouin zone. This 2TA mode is the result of scattering involving two successive first-order TA phonons. The vibrational energy is the sum of these phonons. Therefore, the observed temperature dependence of the shift is also the sum of the shifts in the two one-phonon modes. The shift of the Si-I 2TA mode is less than the TO mode but also exhibits anharmonicity. However, no theory yet exists to describe the temperature dependence of the higher-order phonon scattering processes. It has been noted that the softening of the 2TA phonon mode is indeed mostly due to anharmonic effects rather than lattice expansion.[55]

The main Si-XII line shows a very similar trend to Si-I. However, both the shift and the broadening have a much stronger temperature dependence, which is adequately described by Eqs. (2) and (3) with the higher-order terms omitted. The phonon lifetime at zero temperature is 1.79 ps, which is shorter than that for Si-I (2.84 ps). The fits to Ω of the other Si-XII related lines are also well described by Eq. (2). However, extremely large Ω_o values were required to provide a reasonable fit using Eq. (3). This occurs because the temperature dependence is much weaker than that predicted by the model. This suggests that an additional effect may be operative or the model may be inadequate for describing these phonons. This requires further investigation.

TABLE III. Values for Eqs. (1), (2), and (3) determined by fitting the data in Figs. 2(a)–2(c). All values are in units of cm^{-1}. The errors are from the fits only. The data for the phases marked with an asterisk are shown in Fig. 3.

	Ω_o	A	B	Ω_o[a]	C	D
Fig. 2(a):						
Si-XII	167.92 ± 0.08	-0.63 ± 0.02	0	$(87 \pm 8) \times 101$	2.52 ± 0.08	0
Si-XII	172.4 ± 0.03	-0.49 ± 0.03	0	$(11 \pm 8) \times 101$	2.6 ± 0.1	0
Si-III	186.1 ± 0.1	-0.83 ± 0.03	0	$(14 \pm 4) \times 102$	1.93 ± 0.05	0
Fig. 2(b):						
Si-XII*	362.7 ± 0.2	-4.51 ± 0.09	0	362.7 ± 0.2	2.97 ± 0.02	0
Si-III/XII	385.3 ± 0.2	-5.3 ± 0.1	0		7.08	
Si-III	395.5 ± 0.3	-5.1 ± 0.2	0	$(68 \pm 6) \times 101$	6.4 ± 0.3	0
Si-XII	407.8 ± 0.2	-4.97 ± 0.09	0	$(62 \pm 2) \times 101$	5.2 ± 0.1	0
Fig. 2(c):						
Si-III*	447 ± 1	-4.5 ± 0.6	0			
Si-I TO*	526.8 ± 0.3	-3.2 ± 0.3	-0.17 ± 0.05	526.8 ± 0.3	1.85 ± 0.05	0.02 ± 0.01
Si-I 2TA*	304.3 ± 0.6	-0.4 ± 0.4	-0.10 ± 0.03			

[a]Values required to provide good fits with Eq. (3). Only the Ω_o values for Si-I TO and the main Si-XII lines could be used in both Eqs. (2) and (3).

Given the broad Gaussian line shape of the main Si-III line, there is some scatter in the data for the line shift but it generally shows a strong temperature dependence that is well described by Eq. (2), again with the higher-order terms omitted. In contrast to Si-I and -XII, which can be explained purely with anharmonic phonon-phonon interactions, the linewidth of the main Si-III line decreases with temperature. As a result, we find that Eq. (3) cannot be used with realistic parameters. Therefore, this suggests that the main Si-III phonon is not governed by anharmonic processes.

In the following, we discuss the various possible physical causes of these results. First, intrinsic stresses have been observed to give rise to linewidth sharpening in deposited hydrogenated a-Si.[54] A sharp transition to an anharmonic linewidth broadening regime was observed for measurement temperatures above the deposition temperature. However, for this material, the linewidth is determined by the short-range order. Furthermore, we did not observe such an affect for a-Si formed by indentation. Likewise, such an effect is not expected for Si-III. It is possible that the line shape of additional lines calculated by Piltz *et al.* in the vicinity of the main Si-III line may have temperature dependences such that an artificial sharpening of the main Si-III line shape is observed.[18] However, such lines are not resolved here nor in pressure-dependent studies.[21]

Finally, e-p coupling can result in the narrowing of Γ with increasing temperature, as observed in a broad range of materials from osmium[56] to graphene,[57] to name a few. E-p coupling can lead to a superconducting transition such as in highly B-doped Si-I with a superconducting transition temperature of $T_c = 0.35$ K.[58] Other Si phases also become superconducting when under pressure, such as Si-II with $T_c = 6.3$ K at 12 GPa and Si-V with $T_c = 8.2$ K at 8 GPa.[59] E-p coupling occurs via Landau damping where, in the context of Si-III, the main Si-III phonon may decay into an electron-hole pair rather than lower-energy phonons as supposed by Eq. (3).[60,61] We note that since other Raman lines assigned to Si-III in this study were not observed to sharpen with increasing temperature, the main Si-III line dominates the e-p interaction. In the absence of a well-known energy level diagram, we propose an empirical equation similar to that proposed by Cui *et al.*[35] to describe the linewidth sharpening as a function of temperature. This equation has the form

$$\Gamma(T) = \Gamma_o\left(1 - \frac{F}{\exp(\hbar\omega/k_bT) - 1}\right), \tag{4}$$

where Γ_o and F are fitting parameters. This equation has a similar form to Fermi's golden rule, which has been used to relate the Fermi level and the Raman linewidth broadening due to the e-p interaction.[57,62] This equation fit the data in Fig. 3(b) excellently and yielded the values $\Gamma_o = (16.5 \pm 0.1)\,cm^{-1}$ and $F = 0.8 \pm 0.1$. If this is extrapolated to zero temperature, the phonon lifetime is 0.3 ps.

If we assume that anharmonic effects are negligible, the coupling strength between electrons and the main Si-III phonon, λ, can be approximated via Allen's formula for metals,[40]

$$\frac{\Gamma}{\Omega^2} = \frac{2\pi}{g}\lambda N(E_F), \tag{5}$$

where g is the mode degeneracy and $N(E_F)$ is the phonon density of states at the Fermi level per spin per unit energy per unit cell. The value of Ω is the average phonon linewidth over all q wave vectors. This can only be observed by Raman or IR measurements from a disordered lattice where the wave-vector conservation rules are relaxed. As mentioned above, angular distortions in the tetrahedral bonds in Si-III have been observed, possibly giving rise to the Gaussian Raman line shape. Also, Si-III is a semimetal with hole conduction at around 5×10^{20} cm^{-3} and an indirect band-gap overlap of 0.3 eV.[5] Therefore, the use of Eq. (5) is justified. Since $N(E_F)$ is not yet known for Si-III, the product $\lambda N(E_F)$ can be calculated from the data in Figs. 3(a) and 3(b) for Si-III. We find that $\lambda N(E_F)/g$ displays a weak temperature dependence varying monotonically from 0.11 eV^{-1} at 80 K

to 0.10 eV^{-1} at 300 K. Although our results may indicate an e-p interaction, no features indicative of a superconducting transition temperature, T_c, are observed in the temperature range studied. This agrees with earlier electrical measurements of microcrystalline Si-III, which were performed down to 1.2 K.[5] However, the behavior may be quite different in single-crystal Si-III. If Si-III has a superconducting transition, it may provide a convenient alternative to highly doped Si or other Si phases that require pressure.

V. CONCLUSION

In conclusion, micro-Raman scattering from the metastable high-pressure phases, Si-III and Si-XII, was measured over a temperature range of 80–300 K. Both the Raman shift and the linewidth were found to have a strong dependence on temperature. This allowed the room-temperature peak positions to be accurately determined for these particular indents. The temperature dependence of most of the observed lines was well described by anharmonic considerations. In contrast, this work reports strong evidence that the main Si-III Raman line shape is governed by e-p coupling rather than anharmonic effects. An empirical formula related to e-p coupling was proposed and fit the data well. Although the evidence is strongly in favor of e-p coupling, further experiments are required to identify the electronic structure of Si-III and its coupling channels with phonons to better understand the interaction. The impact of e-p coupling on the electrical properties of a Si-III device would also be of interest since high-field ballistic transport can be effected by scattering from phonons.

ACKNOWLEDGMENTS

This work is supported by a grant from the Australian Research Council. J.E.B. gratefully acknowledges ARC QEII for financial support.

*johnson.brett@jaea.go.jp

†Present address: Semiconductor Analysis and Radiation Effects Group, Japan Atomic Energy Agency, 1233 Watanuki, Takasaki, Gunma 370-1292, Japan.

[1] S. Ruffell, K. Sears, J. E. Bradby, and J. S. Williams, Appl. Phys. Lett. **98**, 052105 (2011).

[2] B. G. Pfrommer, M. Coâté, S. G. Louie, and M. L. Cohen, Phys. Rev. B **56**, 6662 (1997).

[3] S. Ruffell, K. Sears, A. P. Knights, J. E. Bradby, and J. S. Williams, Phys. Rev. B **83**, 075316 (2011).

[4] J. Crain, G. J. Ackland, J. R. Maclean, R. O. Piltz, P. D. Hatton, and G. S. Pawley, Phys. Rev. B **50**, 13043 (1994).

[5] J. M. Besson, E. H. Mokhtari, J. Gonzalez, and G. Weill, Phys. Rev. Lett. **59**, 473 (1987).

[6] G. Weill, J. L. Mansot, G. Sagon, C. Carlone, and J. M. Besson, Semicond. Sci. Technol. **4**, 280 (1989).

[7] R. H. Wentorf Jr. and J. S. Kasper, Science **139**, 338 (1963).

[8] V. Domnich, Y. Gogotsi, and S. Dub, Appl. Phys. Lett. **76**, 2214 (2000).

[9] J. Parker, D. Feldman, and M. Ashkin, Phys. Rev. **155**, 712 (1967).

[10] S. Minomura and H. G. Drickamer, J. Phys. Chem. Solids **23**, 451 (1962).

[11] J. Z. Hu, L. D. Merkle, C. S. Menoni, and I. L. Spain, Phys. Rev. B **34**, 4679 (1986).

[12] J. S. Kasper and R. H. Wentorf Jr., Science **197**, 599 (1977).

[13] M. I. McMahon and R. J. Nelmes, Phys. Rev. B **47**, 8337 (1993).

[14] M. I. McMahon, R. J. Nelmes, N. G. Wright, and D. R. Allan, Phys. Rev. B **50**, 739 (1994).

[15] M. Hanfland, U. Schwarz, K. Syassen, and K. Takemura, Phys. Rev. Lett. **82**, 1197 (1999).

[16] S. J. Duclos, Y. K. Vohra, and A. L. Ruoff, Phys. Rev. B **41**, 12021 (1990).

[17] Y.-X. Zhao, F. Buehler, J. R. Sites, and I. L. Spain, Solid State Commun. **59**, 679 (1986).

[18] R. O. Piltz, J. R. Maclean, S. J. Clark, G. J. Ackland, P. D. Hatton, and J. Crain, Phys. Rev. B **52**, 4072 (1995).

[19] D. Ge, V. Domnich, and Y. Gogotsi, J. Appl. Phys. **95**, 2725 (2004).

[20] A. Zwick and R. Carles, Phys. Rev. B **48**, 6024 (1993).

[21] H. Olijnyk and A. P. Jephcoat, Phys. Status Solidi B **211**, 413 (1999).

[22] C. Ulrich, E. Anastassakis, K. Syassen, A. Debernardi, and M. Cardona, Phys. Rev. Lett. **78**, 1283 (1997).

[23] C. Ulrich, A. Debernardi, E. Anastassakis, K. Syassen, and M. Cardona, Phys. Status Solidi B **211**, 293 (1999).

[24] A. Debernardi, C. Ulrich, M. Cardona, and K. Syassen, Phys. Status Solidi B **223**, 213 (2001).

[25] J. Menendez and M. Cardona, Phys. Rev. B **29**, 2051 (1984).

[26] T. Hart, R. Aggarwal, and B. Lax, Phys. Rev. B **1**, 638 (1970).

[27] M. Balkanski, R. F. Wallis, and E. Haro, Phys. Rev. B **28**, 1928 (1983).

[28] A. Debernardi, S. Baroni, and E. Molinari, Phys. Rev. Lett. **75**, 1819 (1995).

[29] M. Gu, Y. Zhou, L. Pan, Z. Sun, S. Wang, and C. Q. Sun, J. Appl. Phys. **102**, 083524 (2007).

[30] B. Di Bartolo, *Optical Interactions in Solids*, 2nd ed. (Wiley, New York, 1968).

[31] R. A. Cowley, Philos. Mag. **11**, 673 (1965).

[32] P. Klemens, Phys. Rev. **148**, 845 (1966).

[33] M. S. Liu, L. A. Bursill, S. Prawer, and R. Beserman, Phys. Rev. B **61**, 3391 (2000).

[34] J. B. Cui, K. Amtmann, J. Ristein, and L. Ley, J. Appl. Phys. **83**, 7929 (1998).

[35] H. Tang and I. P. Herman, Phys. Rev. B **43**, 2299 (1991).

[36] U. Fano, Phys. Rev. **124**, 1866 (1961).

[37] F. Cerdeira, T. A. Fjeldly, and M. Cardona, Phys. Rev. B **8**, 4734 (1973).

[38] M. Chandrasekhar, J. B. Renucci, and M. Cardona, Phys. Rev. B **17**, 1623 (1978).

[39] P. B. Allen and M. L. Cohen, Phys. Rev. Lett. **29**, 1593 (1972).

[40] P. B. Allen, Solid State Commun. **14**, 937 (1974).

[41] W. E. Pickett and P. B. Allen, Phys. Rev. B **16**, 3127 (1977).

[42] J. E. Bradby, B. Haberl, and J. S. Williams (unpublished).

[43]H. Richter, Z. P. Wang, and L. Ley, Solid State Commun. **39**, 625 (1981).
[44]P. Mishra and K. P. Jain, Phys. Rev. B **62**, 14790 (2000).
[45]R. Alben, D. Weaire, J. Smith Jr., and M. Brodsky, Phys. Rev. B **11**, 2271 (1975).
[46]J. S. Kasper and S. M. Richards, Acta Crystallogr. **17**, 752 (1964).
[47]R. Kobliska, S. Solin, M. Selders, R. Chang, R. Alben, M. Thorpe, and D. Weaire, Phys. Rev. Lett. **29**, 725 (1972).
[48]P. A. Temple and C. E. Hathaway, Phys. Rev. B **7**, 3685 (1973).
[49]J. B. Renucci, R. N. Tyte, and M. Cardona, Phys. Rev. B **11**, 3885 (1975).
[50]M. Hanfland and K. Syassen, High Press. Res. **3**, 242 (1990).
[51]A. Kailer, K. G. Nickel, and Y. G. Gogotsi, J. Raman Spectrosc. **30**, 939 (1999).
[52]S. Ruffell, B. Haberl, S. Koenig, J. Bradby, and J. S. Williams, J. Appl. Phys. **105**, 093513 (2009).
[53]J. E. Smith Jr., M. H. Brodsky, B. Crowder, M. Nathan, and A. Pinczuk, Phys. Rev. Lett. **26**, 642 (1971).
[54]D. M. Bhusari, A. S. Kumbhar, and S. T. Kshirsagar, Phys. Rev. B **47**, 6460 (1993).
[55]V. V. Brazhkin, S. G. Lyapin, I. A. Trojan, R. N. Voloshin, A. G. Lyapin, and N. N. Mel'nik, J. Exp. Theor. Phys. **72**, 195 (2000).
[56]Yu. S. Ponosov, I. Loa, V. E. Mogilenskikh, and K. Syassen, Phys. Rev. B **71**, 220301 (2005).
[57]D.-H. Chae, B. Krauss, K. von Klitzing, and J. H. Smet, Nano Lett. **10**, 466 (2010).
[58]E. Bustarret, C. Marcenat, P. Achatz, J. Kacmarcik, F. Lévy, A. Huxley, L. Ortéga, E. Bourgeois, X. Blase, D. Débarre, and J. Boulmer, Nature (London) **444**, 465 (2006).
[59]K. J. Chang, M. M. Dacorogna, M. L. Cohen, J. M. Mignot, G. Chouteau, and G. Martinez, Phys. Rev. Lett. **54**, 2375 (1985).
[60]P. B. Allen, Phys. Rev. B **6**, 2577 (1972).
[61]P. B. Allen and R. Silberglitt, Phys. Rev. B **9**, 4733 (1974).
[62]M. Lazzeri, S. Piscanec, F. Mauri, A. C. Ferrari, and J. Robertson, Phys. Rev. B **73**, 155426 (2006).